25th ABCM International Congress of Mechanical Engineering
October 20-25, 2019, Uberlândia, MG, Brazil

COB-2019-1187
NUMERICAL INVESTIGATION OF TRANSIENT HEAT CONDUCTION IN A COMPOSITE MEDIUM WITH A CYLINDRICAL HEAT SOURCE

Fabrício José Carneiro Pena
Marcelo José Santos de Lemos
Departamento de Energia – IEME, Instituto Tecnológico de Aeronáutica – ITA, 12228-900 São José dos Campos, SP, Brazil
pena.fabricio@gmail.com
delemos@ita.br

Abstract. *Heat conduction is a well consolidated subject worldwide, however, a thorough knowledge about this phenomena is a matter of paramount importance for the development of several applications. In light of this, the study presented here shows a numerical solution for an unsteady heat conduction in a composite medium with a cylindrical heat source positioned in the first layer. A two-dimensional heat conduction problem was evaluated within an axisymmetric computational domain, which was discretized through the finite element method. As a source term, several values of constant internal heat generation were applied. Therefore, temperature profiles were investigated in radial and axial directions. Further, a pair of thermal insulation materials were added at the top and bottom of the heat source. Results indicated that an appropriate amount of insulation material must be placed in order to assure more heat propagating through the radial direction.*

Keywords: *Unsteady heat conduction, Multi-layer material, Cylindrical heat source, Finite Element Method*

1. INTRODUCTION

Composite materials are commonly encountered in engineering systems as, for instance, in heat exchangers, nuclear and aerospace components, biomaterials and so forth. The capability to combine multiple thermophysical properties into one component is the pivotal factor for choosing multi-layer materials for many applications. Amongst these applications, thermal and thermodynamic systems involve the heat conduction phenomena and, even though this subject seems to be well consolidated, some problems require a considerable amount of knowledge about it. Coupled with the computational improvement, analytical and numerical methods have been arising as the main choices to solve heat conduction problems, instead of the experimental procedures.

Although analytical methods are known for being limited in complex problems, its analysis gives a more insightful understanding of the heat transfer physics. One-dimensional transient heat conduction solutions in a multi-layer region were developed a long time ago and are vastly present in the literature (Carslaw, 1959; Özısık, 1993; Incropera *et al.*, 2007). Y.Gu and O'Neal (1995) used the generalized orthogonal expansion technique to propose an approximate analytical solution in a composite layer with an cylindrical heat source. It has recently been shown that analytical methods are advancing in order to attend more complex applications. As a example, Delouei *et al.* (2012) have proposed an exact analytical solution for an unsteady axi-symmetric conductive heat transfer in a cylindrical orthotropic medium.

Nowadays, most engineering applications demand quick solutions of cases with an high degree of complexity and, for such, numerical methods are the most suggested. These methods grant the solution of cases involving complex three-dimensional geometries, heat generation varying in time and space, boundary conditions with oscillations, thermal properties as a function of temperature and so on. Among the most consolidated numerical methods, the finite element method has proved to be quite effective for the solution of heat conduction problems in several geometries (L.Wilson and E.Nickell, 1966).

Numerical studies about heat conduction in multilayer materials are more focused in direct applications, such as heat exchangers analysis (D.Bauera *et al.*, 2011). However, such analysis has been expanded for other diverses studies. For example, Abdelal *et al.* (2015) proposed a novel method of oil well abandonment using a thermite reaction as a heat source and the effects of heat generated by the reaction onto other layers was studied.

Motivated by the foregoing studies, this paper presents a numerical solution for a transient heat conduction in a composite medium. Also, a cylindrical heat source was considered in the first layer. The problem was evaluated within an axis-symmetric computational domain, which was discretized through the finite element method. The internal heat generations were kept constant in time and space. In order to give a better understanding of the heat conduction phenomena, a pair of thermal insulation materials were placed at the top and bottom of the heat source. The resulting thermal profiles

were investigated and showed that the appropriate insertion of these materials provided a slightly greater heat propagation in the radial direction.

2. METHODOLOGY

2.1 Model Setup

Prior to the description of the governing equations, a schematic model was established to represent the multi-layer cylinder. Figure 1 shows a planar representation of the case.

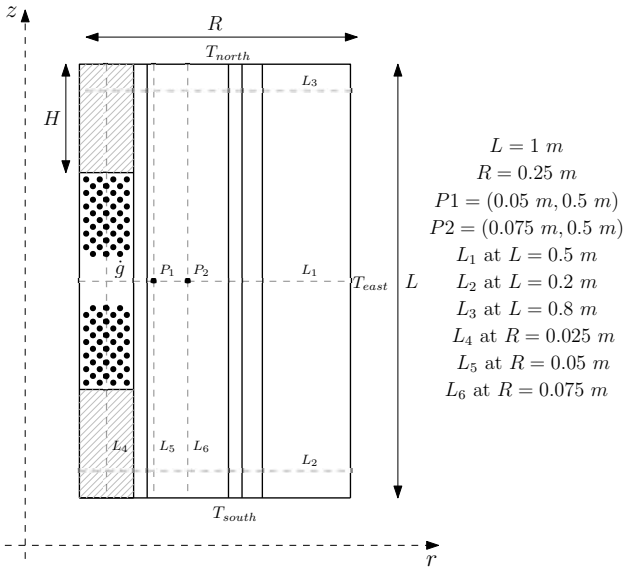

Figure 1: Schematic representation

Analysing the foregoing model, the following assumptions were provided:

(1) Thermal contact resistance between the solids was neglected;
(2) Specific mass, specific heat and thermal conductivity were constant;
(3) Temperature variations through the azimuthal direction were neglected;
(4) At initial conditions, the temperature was uniform throughout the whole domain;
(5) A far-away boundary was considered with a surface temperature, T_s. Thus, the domain was considered semi-infinite.

Accounting these assumptions, the two-dimensional transient heat conduction equation in the first layer can be expressed by:

$$\frac{\partial^2 T(r,t)}{\partial r^2} + \frac{1}{r}\frac{\partial T(r,t)}{\partial r} + \frac{\partial T(z,t)}{\partial z} + \frac{\dot{g}_i(r,z,t)}{k} = \frac{1}{\alpha}\frac{\partial T}{\partial t} \tag{1}$$

where α is thermal diffusivity, which is given by the ratio between the thermal conductivity, k, and the volumetric heat capacity, (ρC_p). In addition, $\dot{g}_i$ stands for the internal heat generation, in W/m^3, while r and z represents, respectively, the radial and axial direction.

As the internal heat generation was considered only in the first layer, this term was not accounted in the remaining ones. Thus, heat conduction through these layers can be described by:

$$\frac{\partial^2 T(r,t)}{\partial r^2} + \frac{1}{r}\frac{\partial T(r,t)}{\partial r} + \frac{\partial T(z,t)}{\partial z} = \frac{1}{\alpha}\frac{\partial T}{\partial t} \tag{2}$$

Initially, a constant temperature was employed for the whole domain, as expressed by the following equation:

$$T_{domain} = 60^o C \qquad \text{for } 0 \leq r \leq R\ ;\ 0 \leq z \leq H\ ;\ t = 0 \tag{3}$$

Similarly, the four boundary conditions were defined as:

$$T_{east} = 60^o C \qquad \text{for } r = R\ ;\ 0 \leq z \leq H\ ;\ t \geq 0 \tag{4}$$

$$T_{north} = 60^o C \qquad \text{for } 0 \leq r \leq R\ ;\ z = H\ ;\ t \geq 0 \tag{5}$$

$$T_{south} = 60^oC \qquad \text{for } 0 \leq r \leq R\ ;\ z = 0\ ;\ t \geq 0 \tag{6}$$

$$-k\frac{\partial T(r,t)}{\partial r} = 0 \qquad \text{for } r = 0\ ;\ 0 \leq z \leq H\ ;t \geq 0 \tag{7}$$

As solids were in perfect contact, interfaces were governed by the following equations:

$$-k_{i-1}\frac{\partial T_{i-1}(r,t)}{\partial r} = -k_i\frac{\partial T_i(r,t)}{\partial r} \tag{8}$$

$$-k_{j-1}\frac{\partial T_{j-1}(r,t)}{\partial z} = -k_j\frac{\partial T_j(r,t)}{\partial z} \tag{9}$$

where subscripts i and j stand for any property variation through the radial and axial directions, respectively. Considering that, Eq.(9) was exclusively employed when the insulation materials were added.

2.2 Layer properties

Any thermal model demands both thermal properties and dimensions of the investigated case. As such, the external radius r, specific mass ρ, thermal conductivity k and specific heat C_p of each layer are shown in Table 1. The properties of the insulation material are also included, however, it is important to reiterate that this material was not considered in all computations.

Table 1: Thermal properties and radius of each layer.

Layers	Radius (m)	Specific mass (kg/m^3)	Thermal conductivity (W/m.^oC)	Specific heat (J/kg.^oC)
1	0.04445	4142	47.88	748.1
2	0.047625	7671	26.08	475.61
3	0.10795	983	0.65	4185
4	0.12065	7800	54.21	448
5	0.14605	2010	0.53	736
6	0.25	2630	3.34	953
Ins.Mat	0.04445	1600	0.335	753

2.3 Numerical method and analysis settings

The numerical approach employed to discretize the governing equations was the finite element method. As such equations described a linear behavior, matrices were solved using a direct scheme. Temperature variations in time were solved by a quasi-steady solution method, which used the Picard-Lindelöf algorithm. Considering that, simulations were run in ANSYS® Academic Research Mechanical, release R1 2019.

Table 1 shows all cases simulated and their respective parameters. Firstly, the internal heat generations were varied and their effects on the temperature distribution were studied. Here, it is important to mention that these generations lasted 300 seconds and, after that, were totally deactivated. For the other case, the height ratio H/L has suffered variations and their impacts were investigated. Time-step sizes used for each time interval are also displayed in the table.

Table 2: Cases simulated and respective parameters used.

Case investigated	$\dot{g}$ (W/m^3)	H/L	Time-step (s)			
			0 to 300 s	300 to 1500 s	1500 to 5000 s	5000 to 10000 s
Effects of heat generation on temperature distribution	3 x 10^7	-	0.25	5	25	50
	4 x 10^7	-				
	5 x 10^7	-				
Effects of H/L on temperature distribution	5 x 10^7	0.1	0.25	5	10	25
		0.2				
		0.3				

2.4 Grid Independency

In order to investigate independency of mesh sizes on the results, simulations made use of the following grid sizes: 9964, 16158, 19024, 29086 and 53576 nodes. Here, computations were run with $\dot{g} = 3\text{x}10^7$ W/m^3 and not considered insulation materials. Also, temperature distributions through radial and axial direction were set as parameters of convergence. For that, temperatures were measured over the lines located at $L = 0.2, 0.5, 0.8$ m and $R = 0.025, 0.05, 0.075$ m, as shown in Figure 1. Due to excessive data, average values of these temperatures were calculated and stored as new variables, $\overline{T}_r$ and $\overline{T}_z$, for radial and axial distributions respectively.

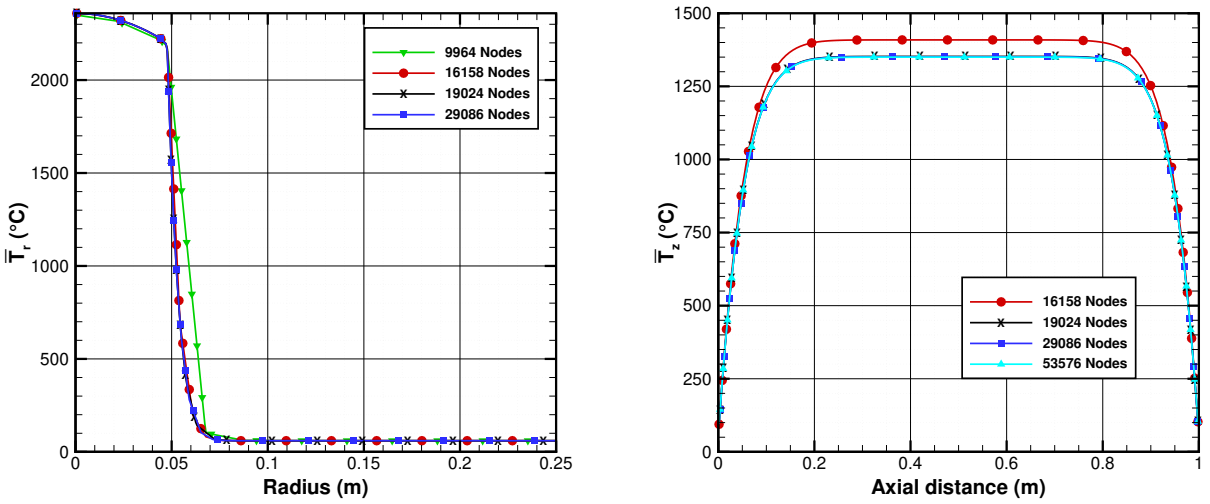

(a) (b)

Figure 2: Temperatures distributions through (a) radial and (b) axial direction. Different grid sizes were considered.

Figures 2a and 2b respectively show the values of $\overline{T}_r$ and $\overline{T}_z$ for different grid sizes. One can observe that $\overline{T}_r$ described converged results with 16158 nodes, whereas $\overline{T}_r$ displayed such behaviour with 19024 nodes. In order to reduce computational costs and still provide a good accuracy, simulations without an insulation material were computed using this last mentioned grid size, which is shown in figure 3a.

Considering the cases with a insulation materials, the only notable difference was a greater refinement next to the material interfaces. As a example, figures 3b shows the grid used for $H/L = 0.2$.

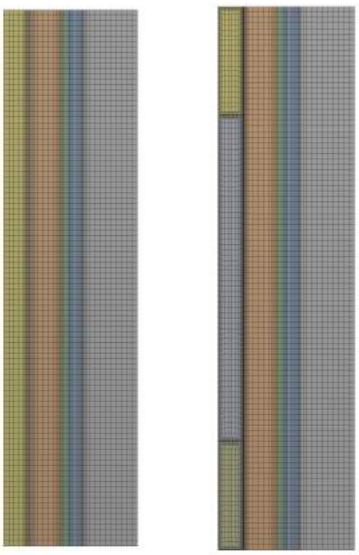

(a) (b)

Figure 3: Grid sizes for (a) the case without insulation material and (b) the case with (b) $H/L = 0.2$.

3. RESULTS

3.1 Effects of heat generation

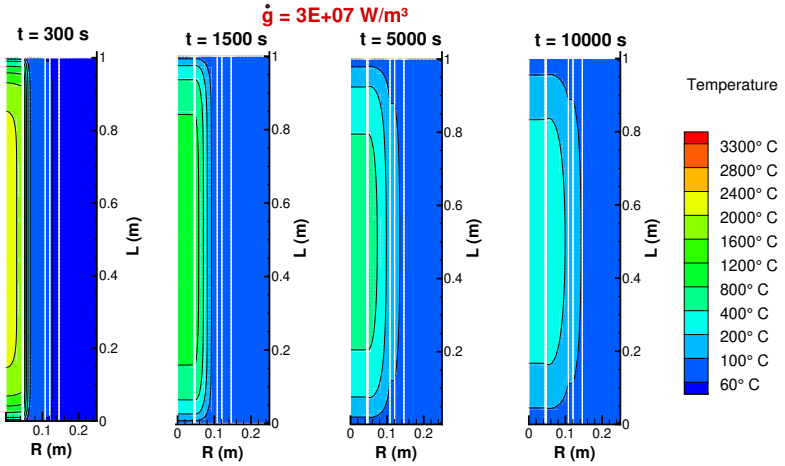

(a)

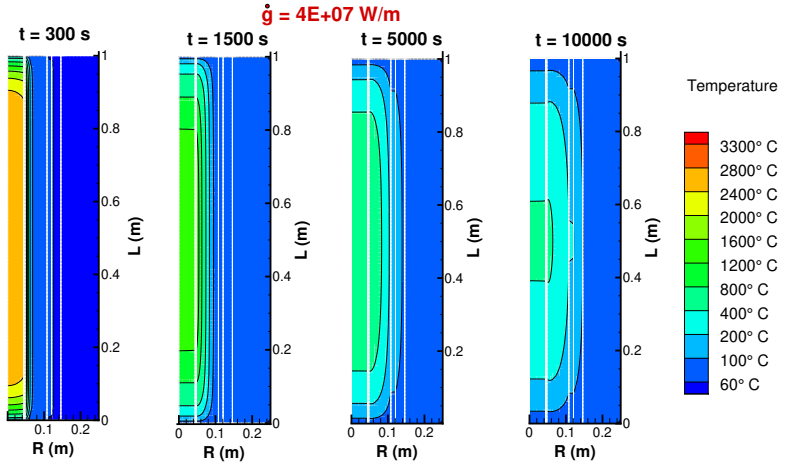

(b)

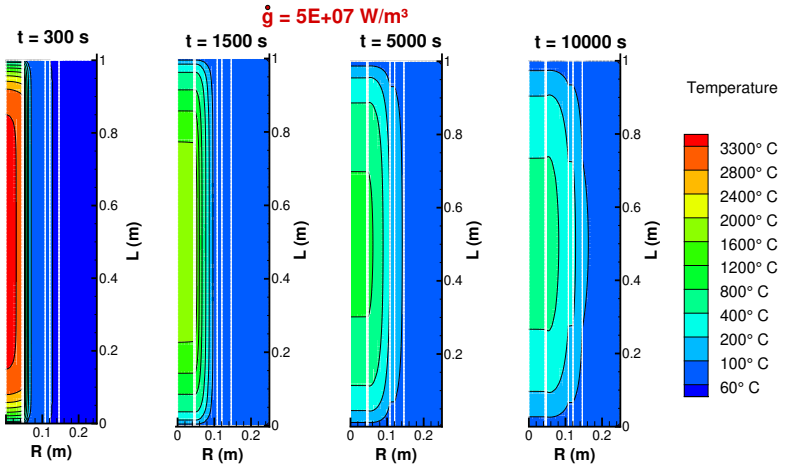

(c)

Figure 4: Temperature contours for $\dot{g} =$ (a) $3\text{x}10^7$, (b) $4\text{x}10^7$ and (c) $5\text{x}10^7$ W/m^3.

Figure 4 shows the effect of internal heat generation on temperature distribution. Temperature contours are plotted in a $r - z$ domain and are analysed at four different times, namely $t = 300, 1500, 5000$ and 10000 s. Each layer interface is represented by a white line. Also, all other parameters were kept constant. Considering that, figure 4a for $\dot{g} = 3$ x 10^7 W/m^3 describes that as time passes, temperatures decrease in regions close to the heat source. On the other hand, the overall temperature enhances at farther distances. Such behavior is in accordance with the governing equations, since time is demanded to heat propagate through the whole domain and reach a thermal equilibrium. Moreover, heat clearly concentrates before the third interface and therefore is possible to presume that the third layer works as an insulation material. As the internal heat generation increases to $\dot{g} = 4$ x 10^7 W/m^3 (Fig.4b), temperatures improves through the whole geometry. Further increasing $\dot{g}$ (Fig.4c), temperatures raise even more, demonstrating coherent results with previous observations in Fig.4a and b.

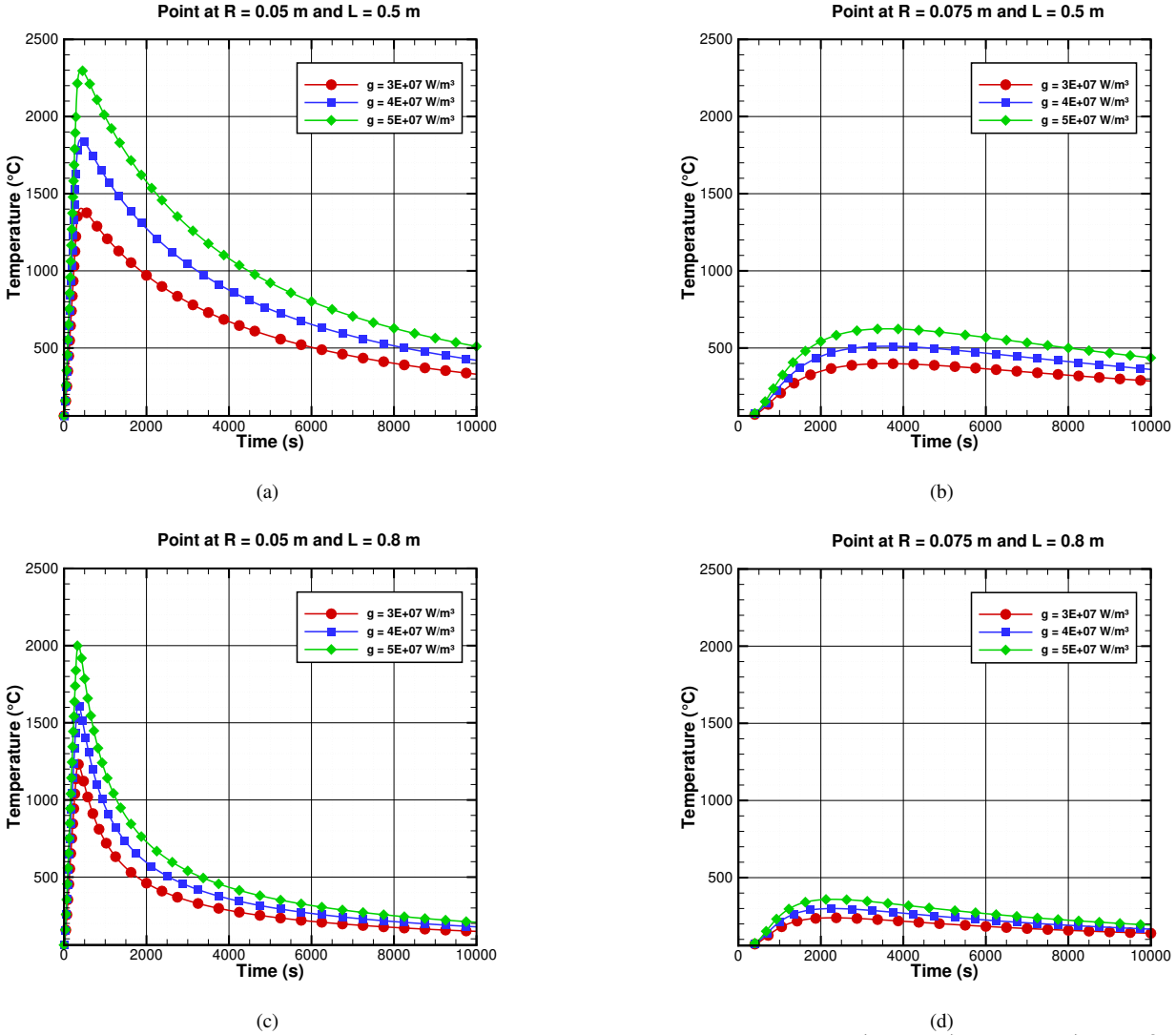

Figure 5: Temperature profiles at (a) P_1,(b) P_2,(c) P_3 and (d) P_4. For $\dot{g} = 3$ x $10^7, 4$ x 10^7 and 5 x 10^7 W/m^3.

Proceeding with the same case, figure 5 displays temperature profiles at different points. Such points are located in the third layer and are also defined in figure 1 as P_1, P_2, P_3 and P_4. It can be observed in Fig.5a, b, c and d that increasing the generation results in higher temperatures, emphasizing the behaviour reported previously. Also, a drastically drop in temperature occurs when the heat propagates through this layer, which can be better observed when comparing the curves in Fig.5a and b or Fig.5c and d. Therefore, the low thermal conductivity material presented in this layer definitely limitates the heat transfer through the radial direction. Finally, a comparison between points at different horizontal positions demonstrates that temperatures were higher next to center (Fig.5a and b), whereas temperatures next to the top surface (Fig.5c and d) were significantly lower. Also, temperatures peaks lasted less next to the top surface, resulting in a quicker cooling down. These results are coherent, since these points were more distant of the heat source.

3.2 Effects of H/L

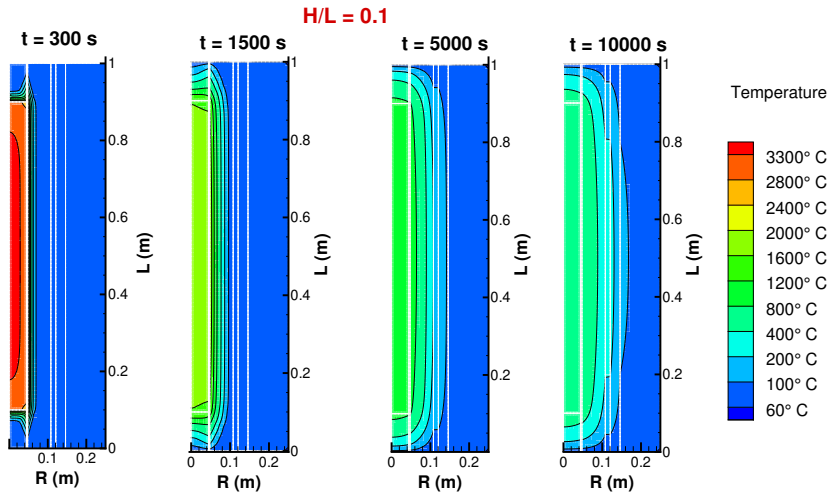

(a)

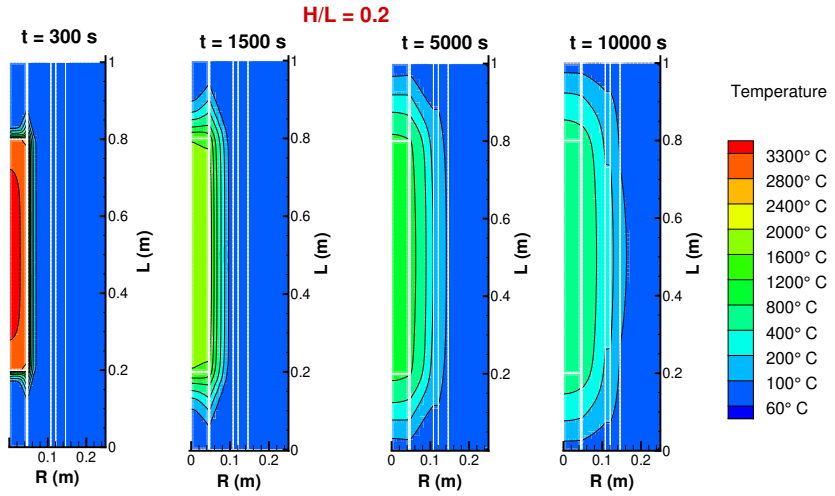

(b)

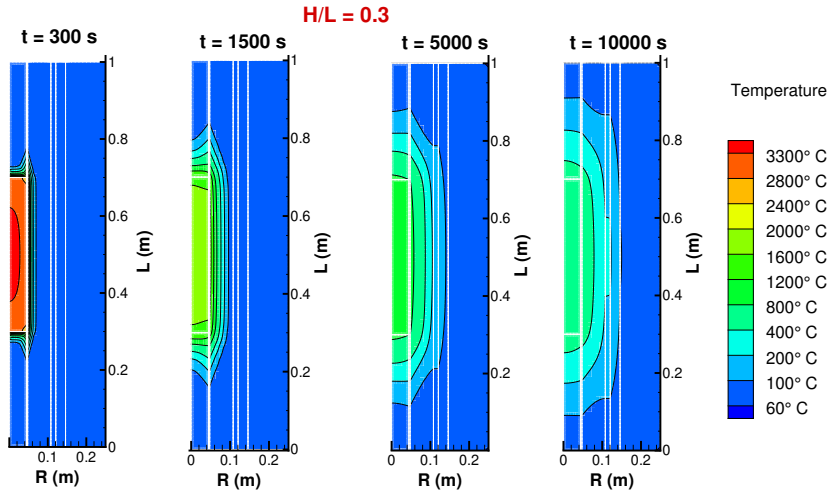

(c)

Figure 6: Effects of insulation materials on temperatures contours. For $H/L =$ (a) 0.1, (b) 0.2 and (c) 0.3.

The effect of the height ratio H/L is presented next. Similarly to a previous analysis, temperatures distributions were analysed at four different times. Also, the case under investigation was simulated with $\dot{g} = 5$ x 10^7 W/m^3 and used height ratios equal to 0.1, 0.2 and 0.3. Having said that, Fig.6a for $H/L = 0.1$ shows that temperatures decrease as time passes, but more importantly, the difficult to heat propagate through the axial direction is clearly elucidated next to the heat source. Therefore, there is an explicit heat concentration in this region. In addition, it is possible to imply that heat achieved far distances than in the case shown in Fig.5c. Further increasing insulation materials sizes also results in an enhancement of heat concentration. However, it is important to mention that the heat propagation reduced through the radial distance, indicating that there might be a ideal quantity of insulation material to be placed.

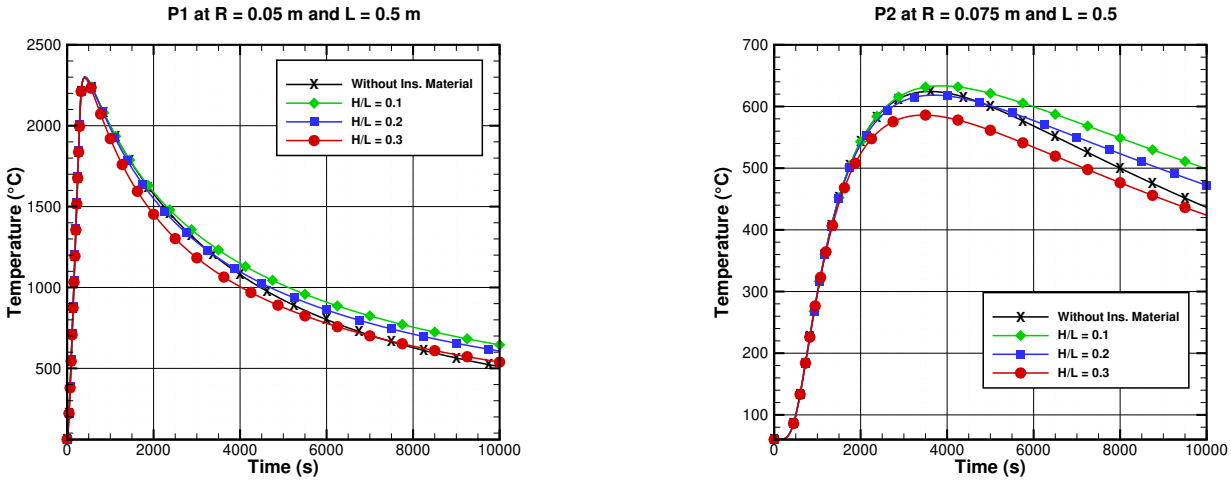

(a) (b)

Figure 7: Effect of insulation materials on temperatures profiles at P_1 and P_2.

Finally, a comparison between cases is described next. Here, temperatures profiles at P_1 and P_2 are shown for all cases run with $\dot{g} = 5$ x 10^7 W/m^3. Considering that, it can be noted in Fig.7a that the implementation of the insulations materials will not affect the peak temperatures. On the other hand, the cooling process for cases with insulations materials is slower and, therefore, at a certain time their temperatures will become higher. At P_2 (Fig.7b), peak temperatures are higher for $H/L = 0.1$, however, further increment of insulation materials does not rise temperatures even more. Therefore, such results reiterate observations stated in the previous topic. One explanation for that behaviour is the reduction of the heat source size and, consequently, the amount of heat emitted by it.

4. CONCLUDING REMARKS

Numerical analysis of unsteady heat conduction in a multilayer configuration was investigated using different internal heat generations and sizes of insulations materials. The reliability of results was evidenced through a grid independency study. It was possible to conclude that temperature distributions behaved accordingly to governing equations and the effects of different layers thermal properties were clearly demonstrated. Also, increasing internal heat generations implied in more elevated temperatures for all analyzed cases. It was also observed that temperatures decreased in the third layer, indicating that such material belongs to the insulation class. Finally, increasing the size of the insulation materials have not necessarily resulted in a stronger propagation through radial direction, which indicates that a certain amount of material must be place in order to achieve such effects.

Results herein might contribute to the design of multilayer applications that desire heat propagating through multiple layers.

5. ACKNOWLEDGEMENTS

This study was financed in part by the Coordenação de Aperfeiçoamento de Pessoal de Nível Superior – Brasil (CAPES) – Finance Code 001. We would also like to show our gratitude to ANSYS, Inc. for providing an academic license.

6. REFERENCES

Abdelal, G.F., Robotham, A. and Carragher, P., 2015. "Numerical simulation of a patent technology for sealing of deep-sea oil wells using nonlinear finite element method". *Journal of Petroleum Science and Engineering*, Vol. 133, pp. 192–200.

Carslaw, H. S.; Jaeger, J.C., 1959. *Conduction of heat in solids*. Oxford: Clarendon Press, 2nd edition.

D.Bauera, W.Heidemanna and H.-J.G.Diersch, 2011. "Transient 3d analysis of borehole heat exchanger modeling". *Geothermics*, Vol. 40, No. 4, pp. 250–260.

Delouei, A.A., Kayhani, M.H. and Norouzi, M., 2012. "Exact analytical solution of unsteady axi-symmetric conductive heat transfer in cylindrical orthotropic composite laminates". *International Journal of Heat and Mass Transfer*, Vol. 55, p. 4427–4436.

Incropera, F., Lavine, A., Bergman, T. and DeWitt, D., 2007. *Fundamentals of heat and mass transfer*. Wiley, 6th edition.

L.Wilson, E. and E.Nickell, R., 1966. "Application of the finite element method to heat conduction analysis". *Nuclear Engineering and Design*, Vol. 4, No. 3, pp. 276–286.

Y.Gu and O'Neal, D.L., 1995. "An analytical solution to transient heat conduction in a composite region with a cylindrical heat source". *Journal of Solar Energy Engineering*, Vol. 117, No. 3, pp. 242–248.

Özısık, M., 1993. *Heat Conduction*. John Wiley Sons, 2nd edition.

7. RESPONSIBILITY NOTICE

The authors F.J.C.Pena and M.J.S de Lemos are the only responsible for the printed material included in this paper.